

Comparison of Accelerated Aging of Silicone Rubber Gasket Material with Aging in a Fuel Cell Environment

Sebnem Pehlivan-Davis,¹ Jane Clarke,¹ Simon Armour²

¹Department of Materials, Loughborough University, Loughborough, Leicestershire LE11 3TU, United Kingdom

²Intelligent Energy, Charnwood Building, Holywell Park, Ashby Road, Loughborough, Leicestershire LE11 3GB, United Kingdom

Correspondence to: J. Clarke (E-mail: J.Clarke@lboro.ac.uk)

ABSTRACT: A polymer electrolyte membrane (PEM) fuel cell stack requires gaskets in each cell to keep the reactant gases within their respective regions. Both sealing and electrochemical performance of the fuel cell depend on the long-term stability of the gasket materials. In this paper, the change in properties and structure of a silicone rubber gasket brought about by use in a fuel cell was studied and compared to the changes in the same silicone rubber gasket material brought about by accelerated aging. The accelerated aging conditions were chosen to relate to the PEM fuel cell environment, but with more extreme conditions of elevated temperature (140°C) and greater acidity. The dilute sulfuric acid accelerated aging solutions used had pH values of 1, 2, and 4. In an additional test, Nafion[®] membrane suspended in water was used for accelerated aging, to more closely correspond to a PEM fuel cell environment. The analysis showed that acid hydrolysis was the most likely mechanism of degradation and that similar degradation occurred under both real fuel cell and accelerated aging conditions. It was concluded that the accelerated aging test is a good one for rapidly screening materials for resistance to the acidic environment of the fuel cell. © 2012 Wiley Periodicals, Inc. *J. Appl. Polym. Sci.* 129: 1446–1454, 2013

KEYWORDS: batteries and fuel cells; ageing; elastomers; rubber

Received 13 June 2012; accepted 14 November 2012; published online 12 December 2012

DOI: 10.1002/app.38837

INTRODUCTION

Seals (gaskets) are required in polymer electrolyte membrane (PEM) fuel cell stacks to separate the reactant gas compartments (hydrogen and oxygen) from each other.

Long-term durability of the fuel cell stack depends on the performance of these gaskets. If the gaskets fail, the reactant gases (H₂ and O₂) can leak to the environment or mix with each other directly in the fuel cell, causing it to malfunction.

The gaskets used as seals in PEM fuel cell are typically elastomeric materials and exposed to an acidic environment, humid air and hydrogen and subjected to mechanical stress.¹ Thus, elastomeric seals should possess sufficient chemical resistance against the chemically active fuel cell environment. In addition, it should be highly flexible to allow compression of the fuel cell stack when a compressive load is applied.

Silicone rubber is one of the most commercially available elastomeric gasket materials for fuel cell applications due to its low cost and ease of fabrication.

There are many published reports based on the degradation of silicone rubbers in various environments.^{2–12} For instance, Patel et al.² carried out a study on the thermal aging of polysiloxane

rubber in both sealed conditions and in open air. Schulze et al.¹³ investigated the degradation of seals in a polymer electrolyte membrane fuel cell during fuel cell operation. Tan et al.^{1,14} studied the degradation of silicone rubber in a simulated PEM fuel cell environment. Chemical and mechanical degradation of the elastomeric materials was also reported in other articles.^{15–20}

Although, there is a large amount of literature discussing the degradation of silicone rubbers in various environments, there are only a small number of results reported for the degradation of silicone rubber in a real PEM fuel cell environment or for degradation using Nafion[®] membrane as an accelerated aging agent.

In this article, we report the results from an investigation of silicone rubber gaskets used in an actual fuel cell and from degradation studies of the same silicone rubber gasket material under accelerated aging conditions. The objectives of this study are to (1) determine the effect of exposure to fuel cell conditions on the silicone rubber gasket, (2) identify potential mechanisms of seal failure, (3) determine the effect of acidity on the rate of silicone gasket material degradation, and (4) determine whether the accelerated aging test could potentially be used to predict degradation behavior in a real fuel cell.

EXPERIMENTAL

Material

A gray-colored polydimethylsiloxane silicone rubber compound filled with silica was used in this study. Samples of new gaskets and gaskets that had been used in fuel cells for various periods were supplied by Intelligent Energy. The same silicone rubber compound was also provided uncured. Sheets of the silicone gasket material (1 mm thick) were cured to 100% in a heated press at 170°C. Dumbbells (Type 2, BS903:Part A2) were cut from the cured sheet for tensile testing before and after accelerated aging. The fuel cell seal gaskets were cured under similar conditions to the sheets.

Characterization Methods

Scanning electron microscopy (SEM) was used to measure the thickness of the silicone rubber gaskets before and after service in the fuel cell. The measurement was used to detect any permanent change in thickness caused by service use. The permanent change in thickness is a similar property to compression set, although the measurement is not carried out under standard conditions, and the level of compression in service is not known. The razor cut surfaces of the unused and used silicone rubber gaskets which had been used in a fuel cell for 5000 and 8000 h were examined using a Carl Zeiss (Leo) 1530 VP SEM.

Atomic force microscopy (AFM) measurements were carried out on the surface of samples cut from both unused gaskets and the degraded part of the used gaskets using a Veeco Explorer AFM with a pulsed force-imaging mode. This technique was used to observe any differences brought about by degradation in the stiffness of the material at a microscopic level.

The atomic composition and surface chemistry of the degraded parts of the silicone rubber gaskets, which had been used in a fuel cell, were identified by applying X-ray photoelectron spectroscopy (XPS). The XPS used in this study was a VG Escalab Mk I with the detection limits of 0.1–1 atom % and an analysis area typically of 3–10 mm².

Attenuated total reflectance Fourier transform infrared (ATR-FTIR) spectroscopy was performed on the surface of the samples from unused and degraded parts of gaskets used in a fuel cell, along with the silicone rubber material before and after exposure to accelerated aging tests. A Shimadzu FTIR-8400S fitted with Specac Golden Gate ATR Mk II was used in this study. The spectroscopy ran at a resolution of 0.85 cm⁻¹ and peak-to-peak S/N ratio of 20,000 : 1.

A solvent swelling method was used to determine the change in the crosslink density of the silicone rubber gaskets on aging. The degree of swelling is inversely related to crosslink density when the material, solvent, and temperature are kept constant, as in this test. Samples with dimensions of 24 × 7 × 0.58 mm³ were cut from unused gaskets and close to the degraded areas of gaskets used in a fuel cell. Each sample was weighed on a digital balance (to four decimal places) then was immersed into a glass tube containing 5 mL solvent (toluene) at room temperature for a total of 6 days. After 1 day (24 h), the swollen sample was removed from the solvent and dabbed on paper tissue to get rid of any excess solvent, placed in a preweighed empty

plastic sample bag and weighed immediately. The sample then was put back in to the glass tube containing toluene for the rest of the swelling test. This procedure was repeated after 24 h (1 day), 96 h (4 days), and 144 h (6 days), and the weights of the samples were recorded. The percentage of swelling was calculated for each sample using the following equation:

$$\text{Swelling (\%)} = \frac{W_2 - W_1}{W_1} \times 100 \quad (1)$$

where W_1 is the weight of the test sample before immersion; W_2 is the weight of the swollen sample after immersion.

Tensile properties were measured for the dumbbell samples both before and after accelerated aging. A Hounsfield universal testing machine fitted with a laser extensometer was used to measure tensile properties. Values of tensile strength, elongation at break and 50% modulus were recorded and the mean values determined. The 50% modulus is a measure of stiffness used for elastomers and is the stress recorded at 50% elongation. Four dumbbells were measured for each aging time.

Accelerated Aging Method

An accelerated aging test was developed in order to assess the acid and time/temperature aging resistance of the silicone rubber, which is relevant to the fuel cell environment. An accelerated aging temperature of 140°C was selected so that 1 week of accelerated aging would roughly correspond to a real life time of 10000 h at 80°C, on the crude assumption of an expected doubling of degradation rate for every 10°C increase in temperature. Accelerated aging solutions were used to represent the acidity of the fuel cell environment. Because of the elevated temperature and aqueous environment it was necessary to carry out the accelerated aging in pressurized vessels. Each pressure vessel included a metal base (stainless steel) for holding a polytetrafluoroethylene (PTFE) lining cup and a screw fitting metal cap with a PTFE lid for sealing. The PTFE liner in which the samples were aged had internal dimensions of 30 mm diameter and 44mm in height. Accelerated aging solution (7 mL) was placed in the liner and four dumbbells of cured silicone rubber were added. The necks of the dumbbell samples were submerged completely into the solution. Figure 1 shows (a) the pressure vessel and (b) the layout of the samples in the liner. The PTFE liner containing the samples was then put into the metal base and sealed tightly with the lined metal cap before placing in the oven at 140°C for the appropriate period.

Accelerated aging solutions with acidity levels of pH 1, pH 2, and pH 4 were prepared by diluting 2M sulfuric acid (H₂SO₄) with distilled water. The pH values of the aging solutions were chosen to create acidity, which is similar to that in a real PEM fuel cell, i.e., pH ranging from 3 to 4,¹⁴ but also to include those of greater acidity to accelerate the aging process. In addition to the sulfuric acid solutions, an acidic environment more closely related to that of the fuel cell, where the acidity is due to the sulfonate groups in the membrane, was created using pieces of Nafion[®] suspended in distilled water. Nafion[®] accelerated aging solution was prepared by using 0.7 wt % of Nafion[®], in 7-mL distilled water, heated in the pressure vessel at 140°C

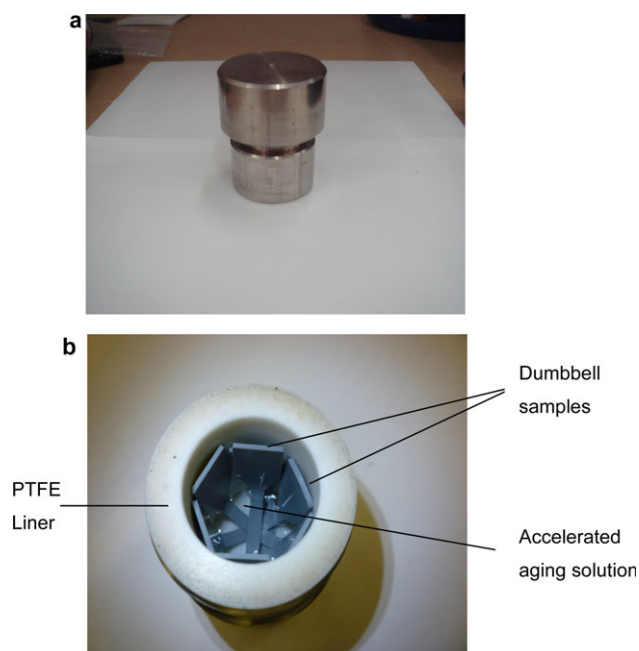


Figure 1. (a) Accelerated aging test pressure cooker and (b) arrangement of the samples in the cooker. [Color figure can be viewed in the online issue, which is available at wileyonlinelibrary.com.]

for 3 days until pH values of between 3 and 4 were reached. The Nafion membrane was left in the water when dumbbell samples were added for accelerated aging.

RESULTS AND DISCUSSION

Scanning Electron Microscopy (SEM)

The individual and average thickness of six samples each of unused and used (5000 and 8000 h) gaskets were measured from SEM images. The mean thicknesses were 580, 622, and 568 μm for the unused, in service for 5000 h and in service for 8000 h samples, respectively. There was a standard deviation of 60 μm for each batch of samples. The results indicate that there was no significant change in the thickness of the gaskets with time and suggest that compression set is unlikely to be a cause of failure for these silicone rubber gaskets.

Atomic Force Microscopy

Silicone gaskets that had been used in a fuel cell showed clear areas of degradation particularly where the edge of the membrane rested against the gasket. Degradation appeared as a white powdery substance on the surface and in some cases the surface was degraded away and holes could be observed. For one of these degraded gaskets, AFM measurements were carried out to determine whether changes in stiffness of the material could be detected where degradation had started but had not progressed

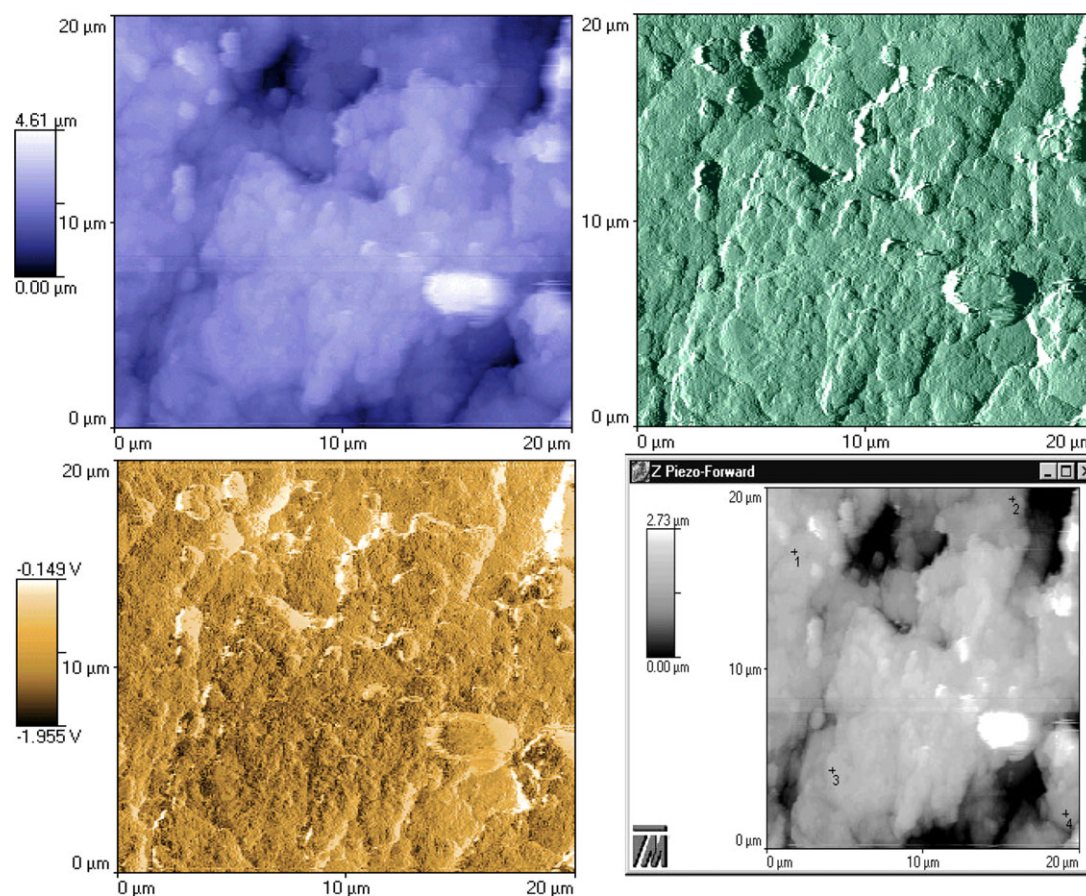


Figure 2. Topographic images of used silicone rubber gasket: Location 4. The points (1, 2, 3, and 4) on right bottom image indicate the points at which AFM modulus was calculated for each location. [Color figure can be viewed in the online issue, which is available at wileyonlinelibrary.com.]

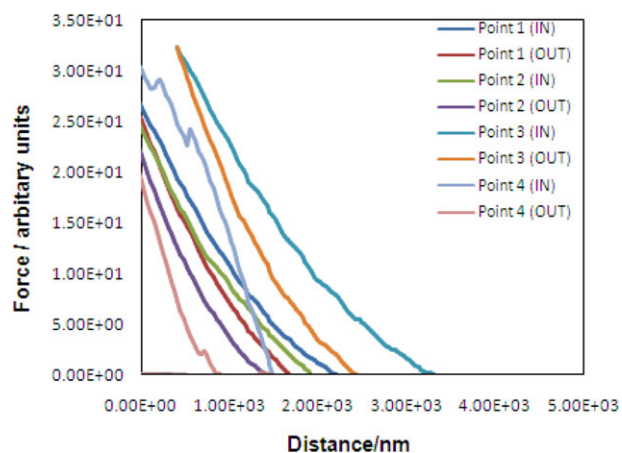


Figure 3. Force/distance curves of the used silicone rubber gasket: Location 4. (In and out represents the force measurement of the AFM probe with the amount of indentation on the surface). [Color figure can be viewed in the online issue, which is available at wileyonlinelibrary.com.]

to a visible degree. The AFM measurement of force/deflection started from a less degraded area of the sample and carried on towards a highly degraded area (i.e., from Location 1, a clean looking edge to Location 5, the area of maximum degradation). At each location, four different points were measured and an AFM “modulus” was then calculated for each location from the slope of the force/distance curves. In addition to these numerical values, images were obtained that also contained qualitative information. An example of these images is given in Figure 2. The top left image of Figure 2 gives information about the height of the surface. The black areas in the picture represent a low point (i.e., a hole) and white parts signify the high points. The top right image is a tip-deflection image with shaded areas in the picture accentuating the edges. The bottom left image is a phase topographic image, which expresses the phase of the reaction related to the force that is applied in the measurement. Darker parts in the image correspond to a lower phase lag and probably indicate the presence of rigid fillers, whereas the light areas could be explained as soft, rubbery parts. Finally, the image on the bottom right illustrates the points at which force/distance curves were acquired (i.e., +1, +2, +3, and +4). Figure 3 shows the force/distance curves, which were measured at four points at Location 4 of the used silicone rubber gasket. The slope of the force/distance curve is taken as the AFM modulus and has arbitrary units. Figure 4 presents the AFM modulus values of unused and used gaskets which were calculated at four points for each location. The AFM modulus for the four points measured at each location are very scattered, showing as great a variation as that observed between the five different locations of supposed differing degradation. The variation in AFM modulus may well be due to local distribution of filler particles rather than differences in level of degradation of the polymer. Hence, these results suggest that AFM is not a useful tool for determining degree of degradation for this particular compound.

X-ray Photoelectron Spectroscopy

The samples for XPS measurements were obtained by cutting pieces from unused silicone rubber gasket and different parts of

a gasket used in a fuel cell, including, undegraded, stained (brown), and degraded (white) areas. Brown areas may indicate the presence of iron oxide on the surface of the gasket, which might be the result of the corrosion of bipolar plates in the fuel cell. On the other hand, white degraded parts might be caused by hydrolysis due the aqueous acidic environment in the fuel cell. The XPS spectra in Figure 5 reveal the presence of carbon (C), oxygen (O), silicon (Si), and a small amount of fluorine (F). The atomic concentration of these elements are also shown in Table I.

It can be seen from Figure 5(b) that the carbon peak is lower and the oxygen peak higher in the degraded area of the used gasket compared to the ones in the spectra of the unused gasket [Figure 5(a)]. This can be observed also from the ratios of C/Si and O/Si shown in Table I. XPS did not detect iron atoms on the surface of the gasket sample and so it is assumed the concentration of iron (Fe) atom was less than 1% (the detection level of this equipment). The presence of fluorine (F) may be due to contamination of the surface of the samples from the membrane.¹⁵ As shown in Table I, the C/Si ratio is lower for the used gaskets than the unused gaskets, but is particularly low for the degraded part of the used gasket. This could be due to the methyl group on the silicone atom being attacked and oxidized to form Si–O bonds. This behavior would also account for the increase of the O/Si ratio with use and degradation of the gasket (Table I). Additionally, hydrolytic breakage of the –Si–O–Si backbone could cause this increase in O/Si ratio.¹⁵

Attenuated Total Reflectance Fourier Transform Infrared Spectroscopy

ATR-FTIR analysis was used to study the change in the surface chemistry of silicone rubber with degradation. Figures 6 and 7

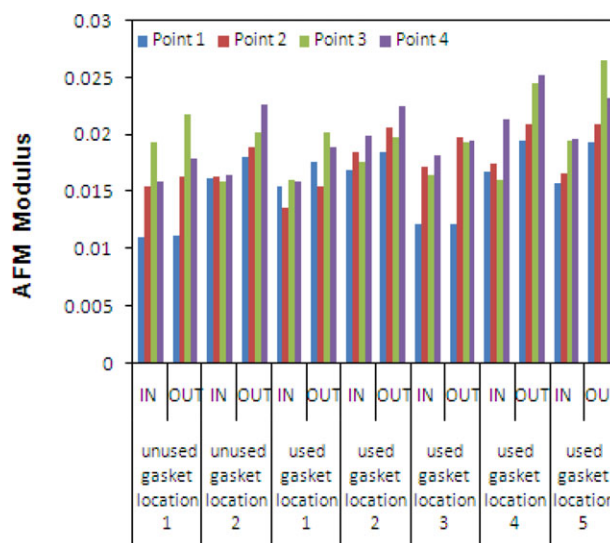


Figure 4. AFM Modulus of unused and used (5000 h in the fuel cell) silicone rubber gaskets (from less degraded area, Location 1, to highly degraded area, Location 5, and at each location four different points were measured). [Color figure can be viewed in the online issue, which is available at wileyonlinelibrary.com.]

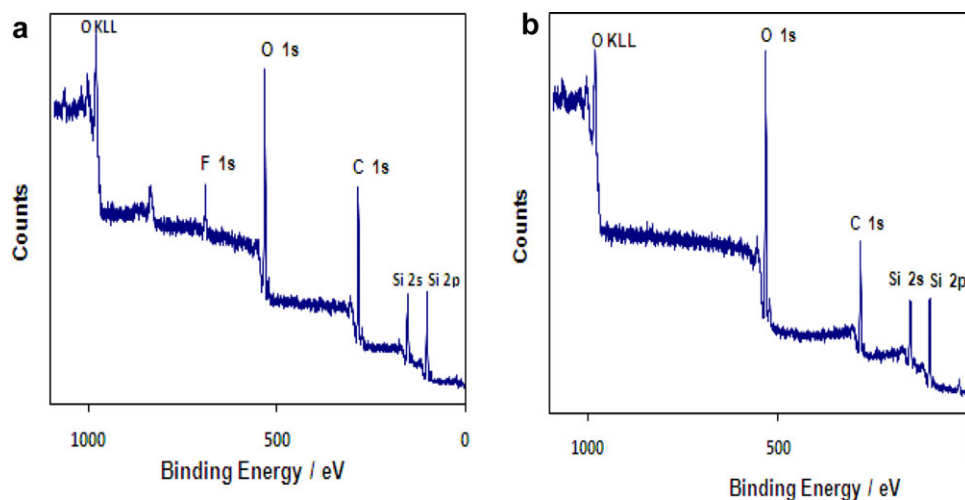


Figure 5. XPS spectra for silicone rubber (a) unused gasket and (b) degraded area of used (5000 h in the cell) gasket. [Color figure can be viewed in the online issue, which is available at wileyonlinelibrary.com.]

show the comparison of the ATR-FTIR results for degraded silicone rubber gasket (operating in the fuel cell for 5000 h) and silicone rubber material after exposure to the accelerated aging test (pH 1 accelerated aging solution for 2 days).

The largest peaks for unused (unexposed) silicone rubber are between 1007 and 1050 cm^{-1} , which are characteristic of siloxanes and associated with asymmetric and symmetric stretching vibrations of Si–O–Si bonds. The peak arising at 694 cm^{-1} is due to the asymmetric deformation of Si–CH₃ bonds.²¹ The peak at 790 cm^{-1} corresponds to the bending mode of Si–C and C–H wagging.²² The peaks at 864 and 1259 cm^{-1} result from the rocking vibration of Si–CH₃ and the bending vibration of Si–CH₃. The peak near 1411 cm^{-1} is due to the rocking vibration of –CH₂– as a part of the silicone rubber crosslinked domain. The peak at 2963 cm^{-1} is related to the stretching vibration mode of CH₃.¹

It can be seen from Figures 6 and 7 that the –CH₂– rocking peak disappeared for the degraded part of the silicone rubber gasket and the silicone rubber material after exposure to accelerated aging. This indicates that crosslinks between the polymer chains were broken during degradation and this might lead to the softening of the silicone rubber. The intensity of the Si–CH₃ bending peak at 1259 cm^{-1} and the peak due to CH at 2963 cm^{-1} decreased significantly in both the degraded silicone rubbers (Figures 6 and 7). This indicates that the methyl (Si–CH₃)

has been hydrolyzed as suggested also by the XPS results. Of particular significance is the similarity of the spectra for the degraded materials from the fuel cell and accelerated aging environment, which means that the accelerated aging conditions bring about a similar type of degradation to that of the real fuel cell environment. A scheme proposing the mechanism of hydrolytic degradation has been included in Tan et al.'s article.¹

Solvent Swelling

Solvent swelling was used to determine whether there were changes in crosslink density brought about by aging of the gaskets. Unused and used gaskets after 5000 and 8000 h service in the fuel cells were analyzed by solvent swelling. After 144 h of swelling in toluene, the percentage changes in volume of the samples were 118, 114, and 109 for the unused, after 5000 and after 8000 h service, respectively. Although the trend suggests a slight decrease in swelling and hence increase in crosslink density, given the very small difference in swelling between the samples in relation to the large amount of swelling of all the samples and a standard deviation of 4 on the swelling measurements, it is considered that the gaskets generally, did not experience significant crosslinking or breakage of crosslinks up to 8000 h in service. The result is a little surprising because both the XPS and the FTIR results indicated that crosslink cleavage and chain scission had occurred in the degraded samples. However, solvent swelling is a bulk measurement, whereas

Table I. XPS Composition in Atom Percentage

Samples	Atomic concentration (%)				Ratios to Si	
	C	O	Si	F	C/Si	O/Si
Unused gasket	50.9	24.2	24.9	Trace	2.04	0.97
Used gasket (undegraded area)	47.2	25.6	25.9	1.3	1.82	0.98
Used gasket (close to stained area)	46.4	26.4	25.5	1.7	1.81	1.03
Used gasket (degraded area)	34.4	35.0	30.6	–	1.12	1.14

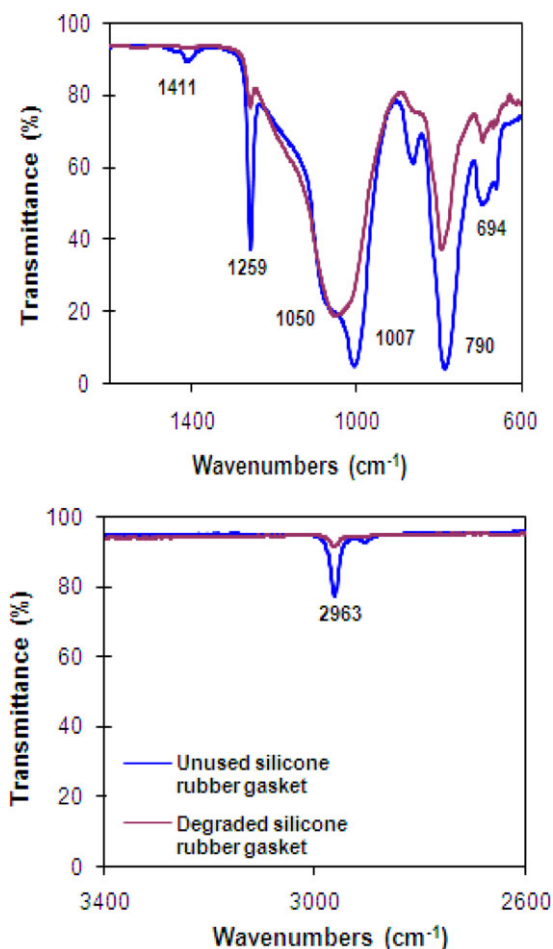


Figure 6. ATR-FTIR spectra after exposure to actual fuel cell environment (comparison of unused silicone rubber gasket with the degraded gasket). [Color figure can be viewed in the online issue, which is available at wileyonlinelibrary.com.]

XPS is a surface technique, and the FTIR was carried out on a sampled piece of rubber exhibiting significant degradation. Considering the swelling and spectroscopic sets of results together, it seems likely that there is little degradation in the bulk of the sample, but severe degradation at the surface.

Accelerated Aging

The surface degradation of the silicone rubber samples before and after exposure to diluted H_2SO_4 aging solution (pH 1, 2, and 4) at different time intervals is shown in Figure 8. It can be seen clearly that the color of the samples in the neck region which was submerged in pH 2 accelerated aging solution started to change from gray to white after 5 days [Figure 11(d)], and the degradation became even more significant (white color in the neck region) after 9 days. The extent of the degradation was more severe in the more highly acidic solution (pH 1); hence, the silicone rubber samples were ruptured in pH 1 solution after only 2 days exposure [Figure 11(b)]. By contrast, there was no sign of the degradation on the surface of the samples after exposure to pH 4 accelerated aging solution for 21 days [Figure 8(h)].

Tensile tests were carried out on these aged silicone rubber samples in order to examine the effect of acid aging on mechanical properties. Figure 9(a–c) shows that tensile strength, elongation at break, and 50% modulus of silicone rubber decreased significantly with time and the rate of decrease was higher in more acidic solutions. The decrease in tensile strength is relatively greater than the decrease in modulus. For example, after 15 days at pH 2, the tensile strength has decreased by 70%, whereas the modulus has decreased by 30%. It is likely that the difference is due to the fact that tensile strength is particularly sensitive to surface degradation while modulus is more of a bulk effect. As was suggested by the swelling and spectroscopic results discussed previously, it seems that severe degradation occurs at the surface but very little occurs in the bulk and as aging progresses the degradation front moves inwards. The thickening of the severely degraded layer, which in itself has very little strength, would inevitably result in a decrease in strength and modulus of the sample due to the smaller amount of undegraded rubber remaining that can take the load. In addition, a brittle degraded layer may also be a site for crack initiation, which would also tend to reduce tensile strength. The particular sensitivity of tensile strength to accelerated aging

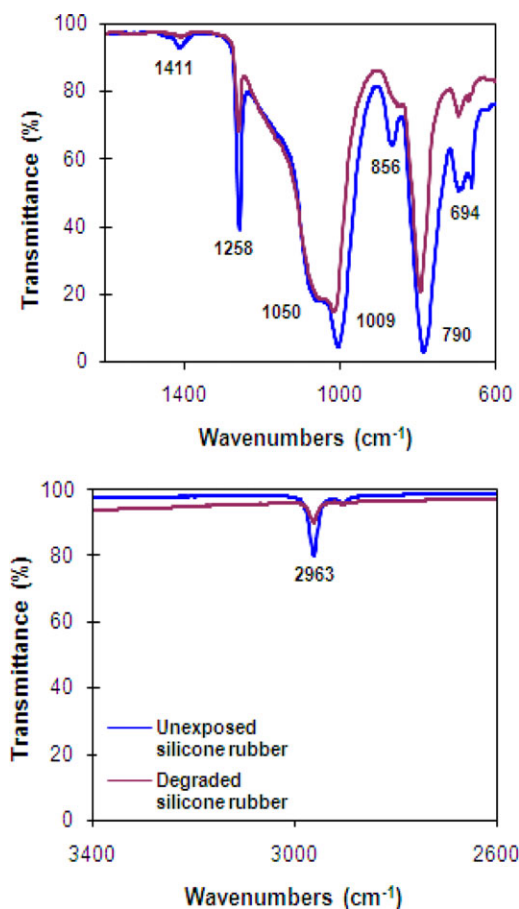


Figure 7. ATR-FTIR spectra after exposure to accelerated aging test (comparison of unexposed silicone rubber with degraded silicone rubber). [Color figure can be viewed in the online issue, which is available at wileyonlinelibrary.com.]

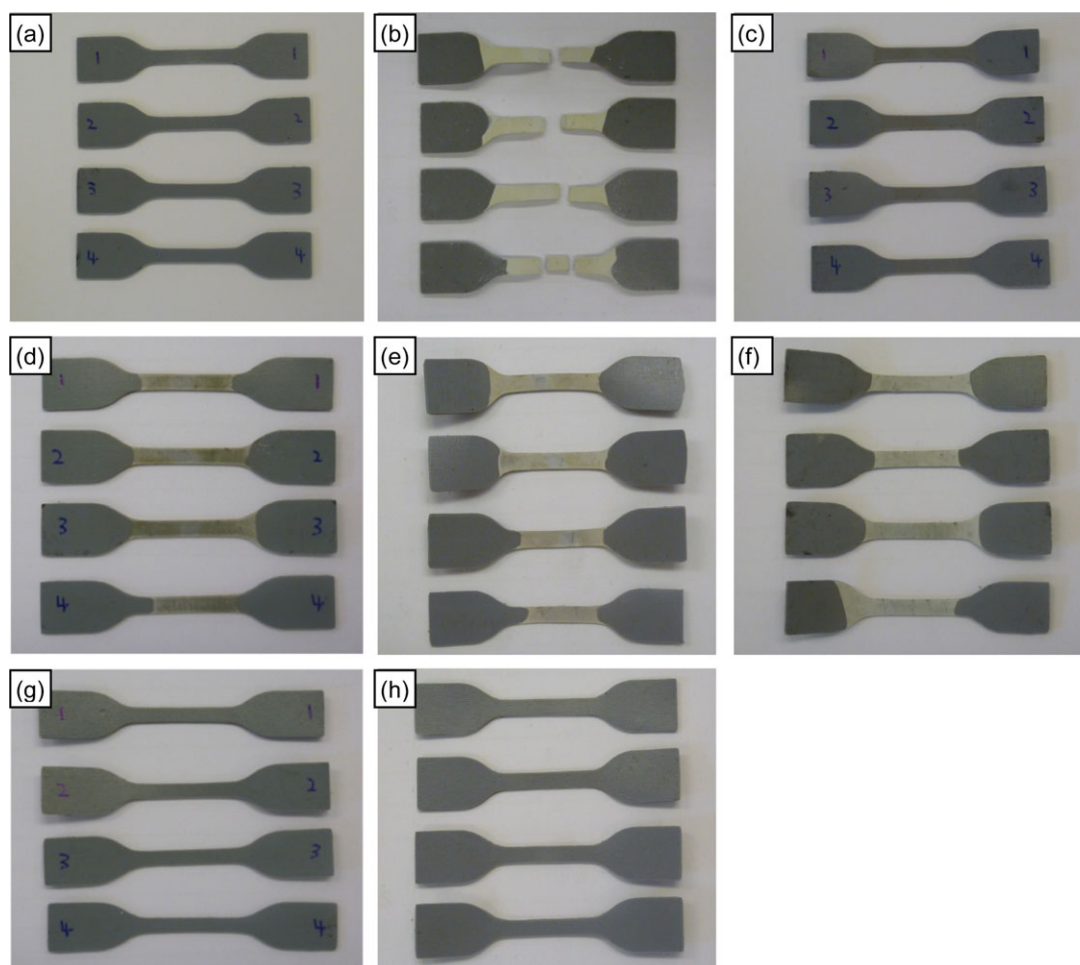


Figure 8. (a) Unexposed silicone rubber, (b) after exposure to pH 1 solution for 2 days; (c) after exposure to pH 2 solution for 2 days, (d) 5 days, (e) 9 days, and (f) 14 days; and (g) after exposure to pH 4 solution for 12 days and (h) 21 days at 140°C. [Color figure can be viewed in the online issue, which is available at wileyonlinelibrary.com.]

makes it a good means of quantifying aging, being much more sensitive and quantitative than the imaging and spectroscopic methods studied. It would have been beneficial to compare these accelerated aging results with the decrease in tensile strength of the gaskets with service life. However, the geometry of the gaskets was not suitable and sites of degradation so localized that a sensible set of tensile data could not be obtained.

Determination of Acidity (pH) Change with Nafion®

The acidity of a PEM fuel cell environment is due to the presence of the sulfonated fluorinated hydrocarbon membrane, and for this reason, it was considered worthwhile to carry out accelerated aging experiments using the membrane as the source of the acid. Nafion® samples, which were cut from different parts of the Nafion® membrane (the edge and central parts), were placed in the pressure vessels containing distilled water and were kept at 140°C for up to 14 days. The weight percentages (wt %) of the Nafion® in water were 0.7 and 1.4.

It can be seen from Figure 10 that despite the differences in the location on the membrane and in amounts used, the pH was found to be consistent, between 3 and 4 over the 14 day

period. Figure 11(a,b) shows the comparison of tensile properties of silicone rubber samples which were exposed to Nafion® aging solution and to the diluted H₂SO₄ solution with pH of 2 and 4 at 140°C for up to 8 days of aging. The standard deviation is less than 0.8 MPa for tensile strength values and less than 50% for elongation at break. It can be seen clearly that the decrease in both tensile strength and elongation at break of silicone rubber, which was aged in Nafion® solution was greater than the one that was aged in diluted H₂SO₄ solution with a pH of 2. The result is surprising since the pH of the Nafion aging solution was higher and so less degradation might have been expected. There is something else coming from the membrane that is accelerating the aging process, or it could be that the membrane in close proximity to the rubber gives locally a lower pH, which degrades the rubber more. Analysis of the Nafion aging solution should be carried out in the future to elucidate possible reasons why the aging is more extreme than in a sulfuric acid solution of similar pH. The assumption that the degree of degradation is solely determined by pH could lead to poor predictions of service life in real fuel cells where Nafion is the source of acidity.

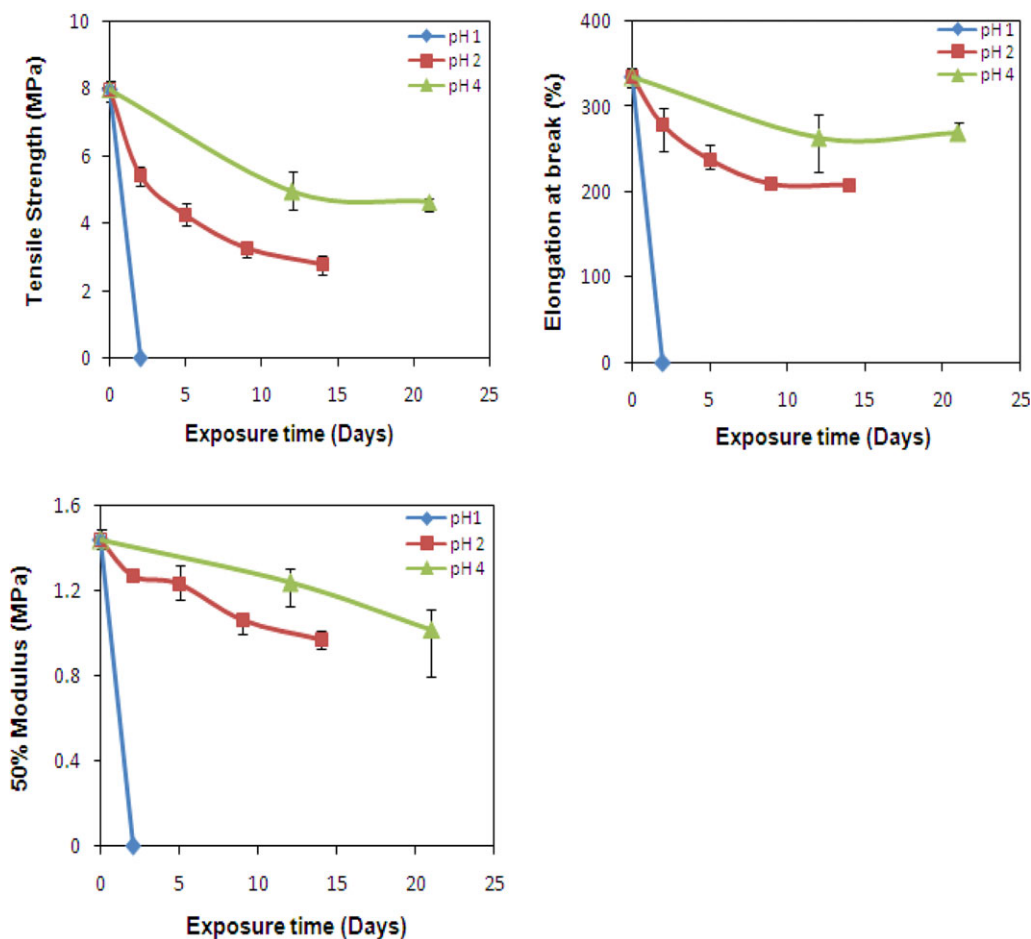


Figure 9. Tensile strength, elongation at break, and 50% modulus of silicone rubber after exposure to acidic solutions of pH 1, pH 2, and pH 4 at 140°C. The error bars indicate plus and minus the standard deviation. [Color figure can be viewed in the online issue, which is available at wileyonlinelibrary.com.]

CONCLUSIONS

Examination of the seals used in the fuel cells for up to 8000 h suggested that failure of the seals would not be due to compression set, but rather due to chemical degradation that made holes in the gasket in places and left a white powdery deposit on the surface in others. Accelerated aging of the same rubber in sulfuric acid solution at 140°C resulted in visibly similar degradation and FTIR analysis of both samples confirming the same type of hydrolysis reactions occurred in both the real fuel cell and accelerated aging test. Greater degradation occurred at lower pH levels confirming acid hydrolysis as the main degradation mechanism. However, aging carried out using hydrated Nafion membrane as the source of acid revealed that there was greater degradation in the presence of Nafion than was achieved with sulfuric acid of the same pH. This suggests that a degradation product from the Nafion membrane accelerates the degradation process in some way. Analysis of the degradation products from the hydrated Nafion should be carried out in future to determine the agent responsible and mechanism by which it achieves degradation of the silicone gasket. AFM proved ineffective as a tool for determining the effect of aging on surface hardness of the rubber, probably because of variations, at a

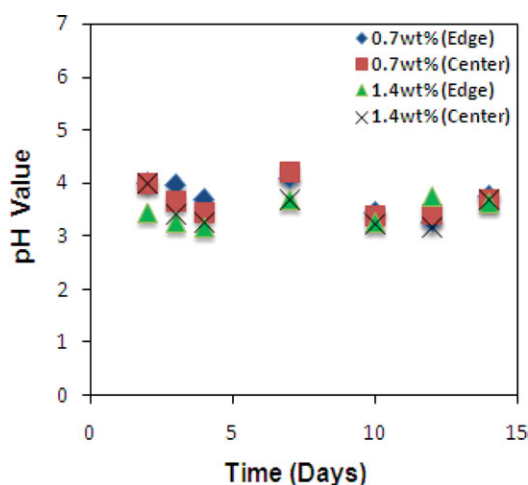


Figure 10. Acidity (pH) change with Nafion® samples taken from different locations on the Nafion® membrane and with different concentrations at 140°C for 14 days. [Color figure can be viewed in the online issue, which is available at wileyonlinelibrary.com.]

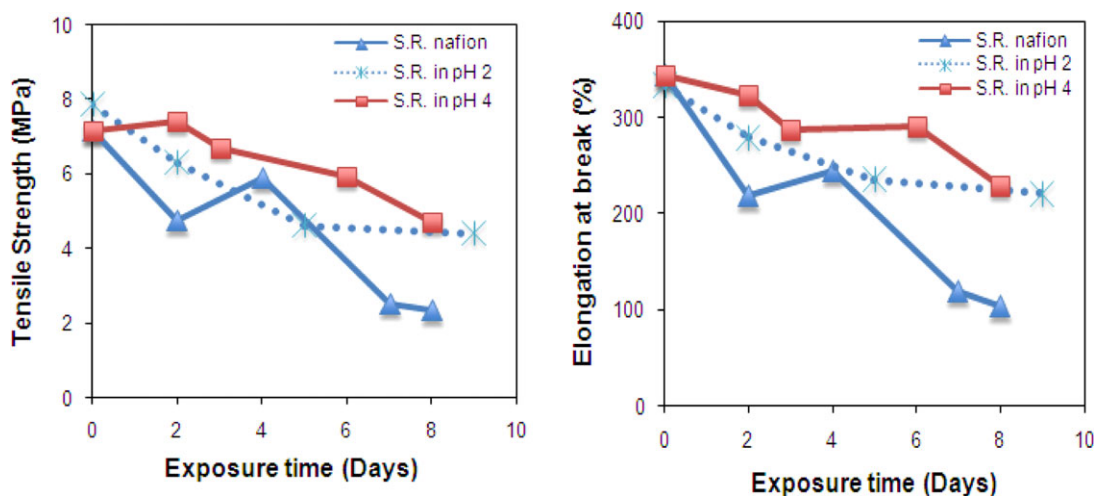


Figure 11. Tensile strength and elongation at break of silicone rubber (SR) after exposure to Nafion®, pH 2, and pH 4 acidic solutions at 140°C. [Color figure can be viewed in the online issue, which is available at wileyonlinelibrary.com.]

microscopic scale, in hardness caused by the presence of filler particles or agglomerates. Solvent swelling tests carried out on the gaskets used in fuel cell seals for up to 8000 h showed an insignificant change in crosslink density while modulus values of the accelerated aging samples showed a relatively small change in modulus compared to the large change in tensile strength. Therefore, it is concluded that the fuel cell seals degrade by acid hydrolysis at the surface exposed to the acid but little degradation occurs in the bulk. Thus, degradation progresses as the degradation front moves inwards from the original surface. The similarity in degradation reactions occurring in the real fuel cells and accelerated aging tests at 140°C means that the accelerated aging tests could potentially be used to predict functional life of silicone seals in real fuel cells. However, such prediction would require that rates of reaction could be shown to follow Arrhenius behavior over the required temperature range. Furthermore, hydrated Nafion should be used as the acid aging agent.

ACKNOWLEDGMENTS

The work was carried out as part of a research project (BH064B) supported by the UK government agency, the Technology Strategy Board (TSB). Encouragement from the industry partners and financial support from the TSB was greatly appreciated.

REFERENCES

1. Tan, J.; Chao, Y. J.; Li, X.; Van Zee, J. W. *J. Power Sources* **2007**, *172*, 782.
2. Patel, M.; Skinner, A. R. *Polym. Degrad. Stab.* **2001**, *73*, 399.
3. Gravier, D.; Farminer, K. W.; Narayan, R. *J. Polym. Environ.* **2003**, *11*, 129.
4. Umeda, I.; Tanaka, K.; Kondo, T.; Kondo, K.; Suzuki, Y. Proceedings of **2008** International Symposium on Electrical Insulating Materials, Yokkaichi, Mie, Japan, Sept. 7–11, 2008, 518.
5. Chaudhry, A. N.; Billingham, N. C. *Polym. Degrad. Stab.* **2001**, *73*, 505.
6. Goudie, J. L.; Owen, M. J.; Orbeck, T. Conference on Electrical Insulation and Dielectric Phenomena, Atlanta, Georgia, USA, Oct. 25–28, **1998**, IEEE Annual Report, 1998, 120.
7. Hillborg, H.; Kornmann, X.; Krivda, A.; Meier, P.; Schmidt, L. E. In Conference on Electrical Insulation and Dielectric Phenomena, Vancouver BC, Canada, Oct. 14–17, 2007; IEEE Annual Report, **2007**, 360.
8. Youn, B. H.; Huh, C. S. *Trans. Dielect. Elect. Insul.* **2005**, *12*, 1015.
9. Liu, H.; Cash, G.; Birtwhistle, D.; George, G. *Trans. Dielect. Elect. Insul.* **2005**, *12*, 478.
10. Gustavsson, T. G.; Gubanski, S. M.; Hillborg, H.; Karlsson, S.; Gedde, U. W. *Dielect. Elect. Insul.* **2001**, *8*, 1029.
11. Yoshimura, N.; Kumagai, S.; Nishimura, S. *Trans. Dielect. Elect. Insul.* **1999**, *6*, 632.
12. Oldfield, D.; Symes, T. *Polym. Test.* **1996**, *15*, 115.
13. Schulze, M.; Knöri, T.; Schneider, A.; Gülzow, E. *J. Power Sources* **2004**, *127*, 222.
14. Tan, J.; Chao, Y. J.; Yang, M.; Lee, W. K.; Van Zee, J. W. *Int. J. Hydrogen Energy* **2010**, *36*, 1846.
15. Tan, J.; Chao, Y. J.; Van Zee, J. W.; Lee, W. K. *Mater. Sci. Eng. A* **2007** 445–446, 669.
16. Tan, J.; Chao, Y. J.; Yang, M.; Williams, C. T.; Van Zee, J. W. *J. Mater. Eng. Perform.* **2008**, *17*, 785.
17. Tan, J.; Chao, Y. J.; Van Zee, J. W.; Li, X.; Wang, X.; Yang, M. *Mater. Sci. Eng. A* **2008**, *496*, 464.
18. Tan, J.; Chao, Y. J.; Wang, H.; Gong, J.; Van Zee, J. W. *Polym. Degrad. Stab.* **2009**, *94*, 2072.
19. Husar, A.; Serra, A. M.; Kunusch, C. *J. Power Sources* **2007**, *169*, 85.
20. Bruijn, F. A.; Dam, V. A. T.; Janssen, G. J. M. *Fuel Cells* **2008**, *8*, 3.
21. Paluszkievicz, C.; Gumuła, T.; Podporska, J.; Błażewicz, M. *J. Mol. Struct.* **2006**, *792–793*, 176.
22. Satoh, K.; Urban, M. W. *Prog. Org. Coat.* **1996**, *29*, 195.